Journal of Mechanical Engineering Research and Developments
ISSN: 1024-1752
Website: http://www.jmerd.org
Vol. 38, No. 2, 2015, pp. 155-162

Three-dimensional Investigations of Vortex Shedding Suppression of A Near-Plane Circular Cylinder in Oblique Flow

C. X. Wang, F. Feng*, & Y. Liu

Collage of Shipbuilding Engineering, Harbin Engineering University, Harbin 150001, Heilongjiang, China

ABSTRACT: In this research, a discussion of results is presented for the dimensionless analysis of generating irreversibility of vessels in which mixing and heating of fluid are done simultaneously. In the first case, the impeller inside the mixing vessel is the heating body, and in the second case heating body is a fixed ring and the impeller inside the vessel. A numerical investigation of flow with various angles past a circular cylinder close to plane boundary has been carried out. Flow equations such as Navier-Stokes equations have been solved using finite volume method. The effects of flow angles on the vortex shedding suppression were investigated with three-dimensional simulation at Reynolds number of $8*10^5$. The angles of incoming flow ranging from 0^0 to 30^0 with an increment of 15^0, each angle was calculated at gap ratios of 0.2, 0.15, 0.1,0.05.The effects of flow angle on vortex suppression were studied, it was found that the effect of angle increases at the critical gap ratio, the vortex shedding is minimized in the oblique flow with angle of 30^0.

KEYWORDS: Vortex shedding; Suppression; Circular cylinder; Flow angle; Numerical simulation.

INTRODUCTION

Flow around a circular cylinder in the vicinity of a plane boundary is one of the phenomena on which our current studies is still far from complete. When fluid flow past a cylinder, vortex shedding occurs. The vortex shedding changes the local pressure on the body each time a vortex sheds from the cylinder, the fluctuating drag and lift force will take place and mounted the cylinder, which may damaging the structure. The cylindrical structures such as subsea pipelines are generally installed on seabed, due to the erosion of the sediment or the brackets of the structure, current past the pipeline has been modeled as flow around a circular cylinder near a plane boundary. Providing predictions on this subject is also frequently applied in offshore/coastal engineering such as submarine cables, stacks, civil engineering such as architectures in the wind, chemical engineering such as coolant past the heater, etc. The possibility of satisfying the practical applications by theoretical knowledge underlies the further research effort in this area.

Bearman and Zdravkovich (1978) [1] carried out the experiment about the flow around the circular cylinder lying horizontally near a plane boundary at Reynolds number Re= $2.5*10^4$, they reported that the vortex shedding suppression occurs for the gap ratio G/D<0.3, with the G being the gap between the bottom surface of cylinder and the plane boundary, D being the cylinder diameter. The Strouhal number was found to be remarkably constant for G/D>0.3.Schewe (1983) [2] reported that the drag and lift coefficients are not sensitive to Reynolds number over a wide range Re of $2.3*10^4$ to $7.1*10^4$. Zdravkovich (1985) [3] continued the work on the flow visualization for Re= $2.5*10^4$, the observation indicated that the vortex shedding suppression still can be observed at the G/D=0.2,the lift coefficient is dominated by G/Din the case of turbulent boundary layer. Taniguchi and Miyakoshi (1990) [4]studied the vortex shedding behavior at Re= $9.4*10^4$, the experimental results indicated that the regular vortex shedding was interrupted at gap ratio is less than 0.3 and the fluctuating lift force increases dramatically beyond the G/D of the vortex shedding starts. Lei et al (1999) [5] investigated the hydrodynamic forces and vortex shedding of a circular cylinder immersed horizontally close to plate over which different turbulent boundary layer at $\mathrm{Re}=1.3\times10^4-1.45\times10^4$, they found that vortex shedding suppressed at about G/D = 0.2 - 0.3 and the drag and lift coefficients both strongly depended on G/D. Furthermore, with the method of Particle Imaging Velocimetry (PIV) technique Price et al. (2002) [6],Wang et al. (2008) [7] and Zang et al. (2013) [8] studied the effect of gap ratio on vortex shedding of circular cylinder above a plane boundary, and presented the decreasing tendency of the swirling strength induced by vortex shedding. Previous experimental studies explored the Reynolds number ranging goes greater and the critical gap ratio of flow characteristics get more progresses in detail.

As the calculation capacity of computer growing rapidly, the numerical simulations were employed continually in this area since 2000, numerical simulations report more convenient and simple predictions on various properties of the flow influence on the cylinder. Lei et al. (2000) [9] solved the Navier-Stokes equations with computational fluid dynamics

(CFD), they demonstrated that the RMS (root mean square) lift force decreased with the decrease of the gap ratio varying from 80 to 1×10^3. A critical gap ratio was reported that the vortex shedding suppressed and the lift force changed dramatically at G/D = 0.2, they also noticed that the effect of Reynolds number is not obvious compared with the gap ratio. These results were well matched their conclusion of their experiment in 1999.Dipankar and Seng up ta (2005) [10] solved the Navier-Stokes equations using an improved overset grid method to research the effect of gap ratios, the computed results such as computed lift and drag coefficients, vortex shedding behavior were compared with the those obtained experimentally by Price et al. (2002) [6], and the computational data matched qualitatively well the experimental data. Zhao and Cheng (2011) [11] investigated the vortex-induced vibration of a circular cylinder close to a plane boundary by RANS (Reynolds-averaged Navier-Stokes) model at the small gap ratios (G/D<0.3 or 0.2).Furthermore, Ong et al. (2010, 2012) [12, 13] stimulated turbulence affected on the circular cylinder placed near a plane at a very high Reynolds number 0.5×10^6 to 3.6×10^6 with standard $k-\varepsilon$ model, they obtained a good prediction of flow and demonstrated that the critical value of G/D is between 0.10 and 0.15 and there is no vortex shedding when the gap is less than 0.1D.

The phases of circular cylinder near plane in the fluid flow have been studied experimentally and numerically for Re = $O(10^2)$ to $O(10^6)$, the principle can be summarized that both the vortex shedding suppression and hydrodynamic forces strongly depend on the gap ratio and weakly on the Reynolds number, the vortex shedding suppression increases as the G/D decreases. However, in reality the incoming flow is not always perpendicular to the cylinder axis, the study of flow with various angles around a circular cylinder near plane is relatively rare. The experimental study of Zhou et al. (2010)[14] and the numerical study of Lam et al. (2010) [15] showed that the error of the principle increases with increasing angle. Thapa et al. (2014) [16] investigated the vortex shedding flow in the wake of a yawed cylinder near plane with three-dimensional simulation. The simulation carried out at two gap ratios of 0.4 and 0.8, yaw angles ranging from 0° to 60°, a constant Reynolds number is 500. It is reported that the mean drag and lift coefficients increase with G/D, the mean drag coefficient reaches its minimum at 15° for G/D=0.4. The low Reynolds number Re=500 allows the direct numerical simulations (DNS), nevertheless, it is not even close to the engineering applications substantially.

GOVERNING EQUATIONS AND NUMERICAL METHOD

The governing equations for simulating the turbulent flow is unsteady impressible Reynolds-Averaged Navier-Stokes (RANS) equations, which can give a good prediction when we are normally interested in the forces on a body. A Cartesian coordinate system is fixed at the center of the circular cylinder and y-axis is perpendicular to the flow direction. The Navier-Stokes equations can be formed into RANS in Cartesian coordinate system as

$$\frac{\partial \overline{u_i}}{\partial x_i} = 0 \tag{1}$$

$$\frac{\partial\left(\rho\overline{u_i}\right)}{\partial t} + \frac{\partial}{\partial x_i}\left(\rho\overline{u_i}\,\overline{u_j} + \rho\overline{u_i`u_j`}\right) = -\frac{\partial \overline{p}}{\partial x_i} + \frac{\partial}{\partial x_j}\left[\mu\left(\frac{\partial \overline{u_i}}{\partial x_j} + \frac{\partial \overline{u_j}}{\partial x_i}\right)\right] \tag{2}$$

where $x_1 = x, x_2 = y, x_3 = z$, are the Cartesian coordinate system in the in-line and the transverse directions of the flow respectively, μ_1 the mean velocity component in x_i direction, tis the time, $\rho\overline{u_i`u_j`}$ is the Reynolds stress, ρ is the fluid density, *p* is the mean pressure, μ is the kinetic viscosity, $\mu(\partial\overline{u_i}/\partial x_j + \partial\overline{u_j}/\partial x_i)$ are the mean viscous stress tensor components. The standard $k-\varepsilon$ model is used for modeling the turbulent flow. Ali et al. (2014) [17] compared all the turbulence models with the experimental data, it was found that for the high Reynolds number scour process modelling, Standard k-ε turbulence model is widely acceptable for its better accuracy and does not require high computational cost. The k and ε equations are given by:

$$\frac{\partial k}{\partial t} + u_j\frac{\partial k}{\partial x_j} = \frac{\partial}{\partial x_j}\left(\frac{\mu}{\sigma_k}\frac{\partial k}{\partial x_j}\right) + \mu\left(\frac{\partial u_i}{\partial x_j} + \frac{\partial u_j}{\partial x_i}\right)\frac{\partial u_i}{\partial x_j} - \varepsilon \tag{3}$$

$$\frac{\partial \varepsilon}{\partial t}+u_j\frac{\partial \varepsilon}{\partial x_j}=\frac{\partial}{\partial x_j}\left(\frac{\mu}{\sigma_\varepsilon}\frac{\partial \varepsilon}{\partial x_j}\right)+C_1\frac{\varepsilon}{k}\mu\left(\frac{\partial u_i}{\partial x_j}+\frac{\partial u_j}{\partial x_i}\right)\frac{\partial u_i}{\partial x_j}-C_2\frac{\varepsilon^2}{k} \tag{4}$$

where ε is the rate of viscous dissipation and μ is defined as $C_\mu k^2/\varepsilon$, the model constants have been adopted: $C_1=1.44$, $C_2=1.92$, $C_\mu=0.09$, $\sigma_k=1.0$, $\sigma_\varepsilon=1.3$. The boundary conditions for the governing equations are given by:

(I) At the non-slip walls and the cylinder surface zero velocity components are specified, the initial values of the pressure in the entire domain are set to zero. The symmetry boundary condition is applied on the top and lateral boundary. The boundary layer thickness at the inlet boundary is the same as the height of the computational domain in the y-direction. All the surfaces of the cylinder and the plane are assumed to be smooth.

(II) The dimensionless velocity at the inlet boundary is written by

$$\left(u_x,u_y,u_z\right)=\left[V(y)\cos a,\ 0,\ V(y)\sin a\right] \tag{5}$$

where the magnitude of the velocity V(y) at the level y^+ is developed based on the velocity of the boundary layer. a is the angle between incoming flow and x-axis (see Figure 1).

$$U^+=\begin{cases} y^+, & y^+\le 11.63 \\ \frac{1}{\kappa}\ln(9.0y^+), & y^+>11.63 \end{cases} \tag{6}$$

$$k=3/2[0.16(Re)^{(-1/8)}\bar{v}]^2 \tag{7}$$

$$\varepsilon=C_\mu^{3/4}\frac{k^{2/3}}{0.07D} \tag{8}$$

where U^+ is defined as $U^+=V(y)/\mu_f$, μ_f is the friction velocity, $y^+=yu_f/\mu$ is the non-dimensional distance from the wall, κ is von Karman constant, its value is confined to be 0.4 ± 0.02 by Bailey et al. (2014)[18]. D is the diameter of the cylinder, Re is Reynolds number which depended on the flow velocity, cylinder diameter and fluid viscosity.

(III) At the outlet boundary, the gradient of the velocity in the direction normal to the boundary is set to zero, the value of the pressure is set to be zero.

The geometry of the computational flow field is schematic in Figure 1. The length of the rectangular flow domain is 20 diameters, the circular cylinder is located at 10D from the inlet boundary, the height from the bottom to the top lateral boundary is 10D. Based on the work by Zhao et al. (2013) [19], the length of the cylinder should be 19.2 diameters to present oblique flow past along the cylinder, hereby the cylinder is set to 20D.

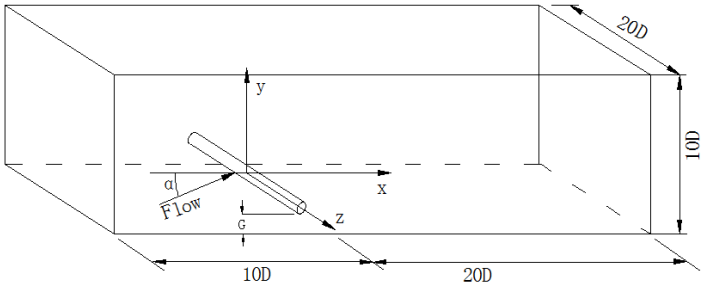

Figure 1. Layout of the flow domain.

The cases are calculated with a non-dimensional time step Δt=0.005, tests have shown this time step is small enough to minimize effects of the time-step. The calculation procedure is 300 to ensure the results are not affected by the calculation time remarkably. The numerical results is obtained base on the t≥100, the data from 0≤t≤100 is reserved in Figures 4-6.Computational mesh of the flow domain is shown in Figure 2, a mesh dependence study has been carried out to ensure the influence of mesh size is little on the results.

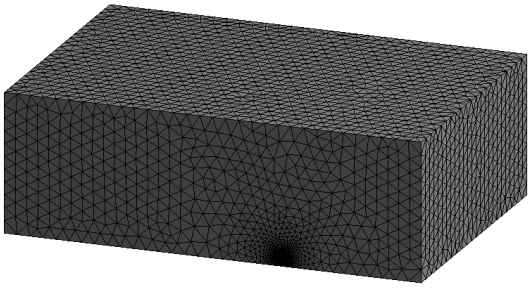

Figure 2. The computational mesh lf the flow field.

RESULTS AND DISCUSSIONS

Numerical investigations were carried out at Reynolds number of $\mathrm{Re}=8\times10^5$, the incoming flow angles of 0 º, 15 °and 30 ° were investigated at each gap ratios of 0.05, 0.10, 0.15,0.20, the effects of angles on vortex shedding will be discussed in the following.

In the case of the flow angle α=0 º, Chen et al. (2013) [20] carried out the experiment of flow around an oscillated and stationary circular cylinder placed near a plate at $\mathrm{Re}=2\times10^5$, the experimental data revealed that vortex shedding suppression occurs at all gaps less than 0.3D. Ong et al. (2012) [13] reported the critical gap ratio for vortex shedding is 0.10≤G/D≤0.15 at $\mathrm{Re}=3.6\times10^6$ .In this study, the critical G/D is expected to be smaller than 0.3 and greater than 0.15.The streamlines were described base on the data obtained at t=300 in Figure 3. It has been shown in the Figure 3a that the vorticities were suppressed at G/D=0.15 in the flow with α=0 º, the upstream encounters the downstream at the back of the cylinder. For G/D=0.20 (see Figure 3b), the wake parallels each other at the back of the cylinder, the vortex shedding occurs, but not strongly. Figures 3a and b reveal the critical gap ratio is between 0.15 and 0.20, which is slightly greater compared with the results from Ong et al. (2012) [13] reported. It is seen in Figure 3d and f that the vorticities are suppressed at G/D=0.2 when the flow with 15 °and 30 °past around the cylinder. At the G/D=0.15 (see Figures 3c and e), the vorticities are also suppressed. It is clearly shown in Figure 3 that the vortex shedding was significantly affected as the flow angle increases.

We may figure out the critical gap ratio through the schemata of the wake, but it is not readily to predicate which angle put a stronger disturbance on vortex shedding. Lei et al. (2000) [9] employed the lift coefficient to represent the vortex shedding, it was found that the amplitude of the fluctuating lift coefficient reduces as the decrease of the gap ratio and the regular oscillation vanishes at the gap ratio for vortex shedding fully suppressed. The lift coefficient is defined as:

$$C_l = \frac{F_l}{1/2\rho D(V(y)\cos\alpha)^2} \tag{9}$$

where F_l is the lift force which acting on the cylinder in the transverse direction. Figure 4a shows that when the incoming flow perpendicular to the longitudinal direction of the cylinder, the lift coefficient fluctuates with a specific frequency at G/D=0.20, which is a good match with Figure 3b. For G/D=0.15, the lift coefficient is mounted irregularly, the vortex shedding is fully suppressed at G/D≤0.10 in as much as the regular oscillation of the lift coefficient completely disappear, which have been shown in Figures 4c and d. Hereby, 0.10≥G/D≥0.15 is the critical area for the vortex shedding strongly suppressed turns to fully suppressed in the case of the incoming flow with an angle 0 º. For the flow with α=15 º, the vorticities are strongly suppressed at G/D= 0.15~0.20 (see Figures 5a and b) and fully suppressed at G/D≤0.10 (see Figures 5c and d).

F_l is the lift force which acting on the cylinder in the transverse direction. Figure 4a shows that when the incoming flow perpendicular to the longitudinal direction of the cylinder, the lift coefficient fluctuates with a specific frequency at G/D=0.20, which is a good match with Figure 3b. For G/D=0.15, the lift coefficient is mounted irregularly, the vortex shedding is fully suppressed at G/D≤0.10 in as much as the regular oscillation of the lift coefficient completely

disappear, which have been shown in Figures 4c and d. Hereby, 0.10≥G/D≥0.15 is the critical area for the vortex shedding strongly suppressed turns to fully suppressed in the case of the incoming flow with an angle 0°. For the flow with α=15°, the vorticities are strongly suppressed at G/D= 0.15~0.20 (see Figures 5a and b) and fully suppressed at G/D≤0.10 (see Figures 5c and d).

Although the lift coefficient of 30^0 flow performs much similarly to the 15^0 flow at G/D=0.20 and 0.15 (see Figures 6a and b), it is noticeable that the amplitude of the former is larger than the latter, that indicates the vortex shedding suppression is stronger in the oblique flow with an angle of 15^0 than 30^0 .As shown in Figure 6c and d, the influence of flow angle is rather weak on gap ratios less than 0.01.

CONCLUSIONS

In this numerical study of vortex shedding and forces of a near-plane circular cylinder in oblique flow, the 3D Navier-Stokes equations for turbulent flow has been solved. The problem of the effects of flow angles on vortex shedding and mean forces coefficients was studied at very small gap ratios (0.02 to 0.2) with flow angles of 0^0 , 15^0 , 30^0 . The results obtained are:

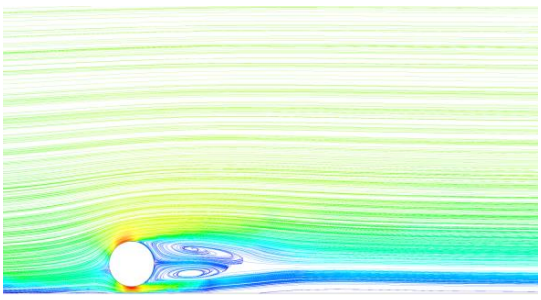

(a)The streamline of G/D=0.15, α=0 °.

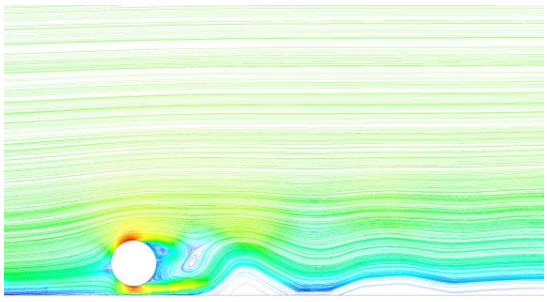

(b) The streamline of G/D=0.20, α=0 °.

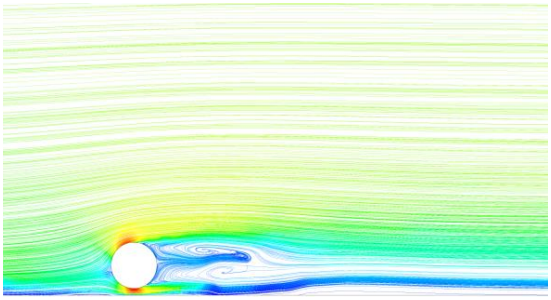

(c) The streamline of G/D=0.15, α=15 °.

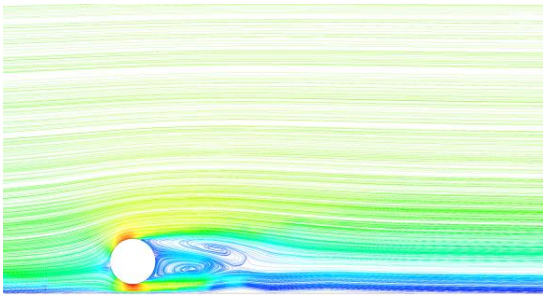

(d) The streamline of G/D=0.20, α=15 °.

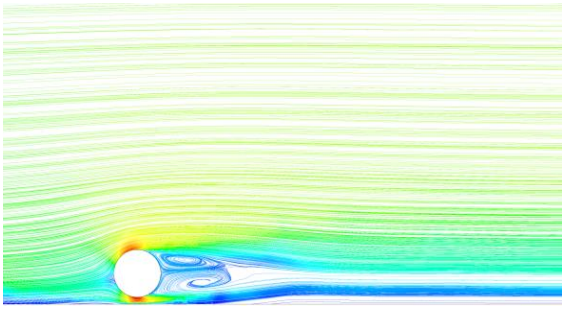

(e) The streamline of G/D=0.15, α=30 °.

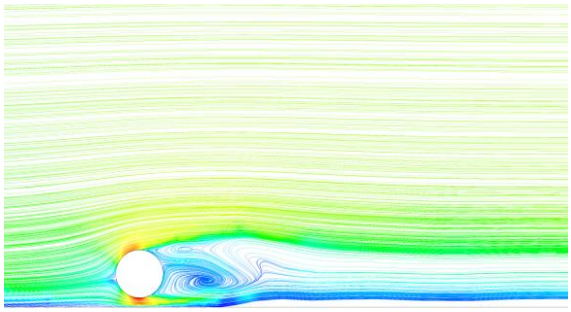

(f) The streamline of G/D=0.20, α=30 °.

Figure 3. The streamline of (a) G/D=0.15, α=0 °, (b) G/D=0.20, α=0 °, (c) G/D=0.15, α=15 °, (d) G/D=0.20, α=15 °, (e) G/D=0.15, α=30 °, (f) G/D=0.20, α=30 °.

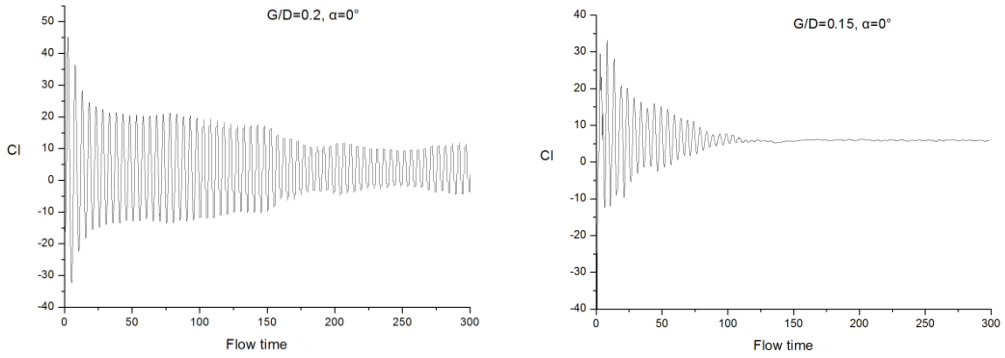

(a) Lift coefficient of G/D=0.20, α=0°. (b) Lift coefficient of G/D=0.15, α=0°.

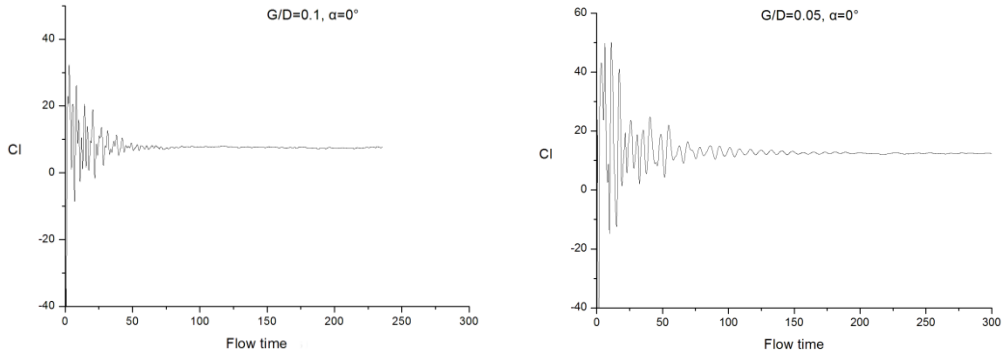

(c) Lift coefficient of G/D=0.10, α=0°. (d) Lift coefficient of G/D=0.05, α=0°.

Figure 4. The lift coefficients of (a) G/D=0.2, α=0 °, (b) G/D=0.15, α=0 °, (c) G/D=0.10, α=0 °.

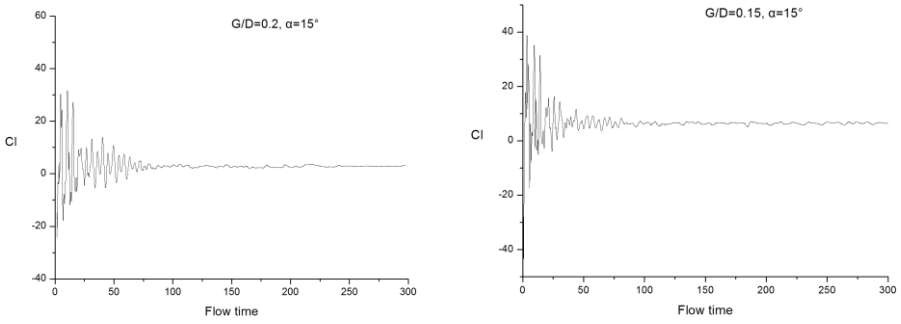

(a) Lift coefficient of G/D=0.20, α=15°. (b) Lift coefficient of G/D=0.15, α=15°.

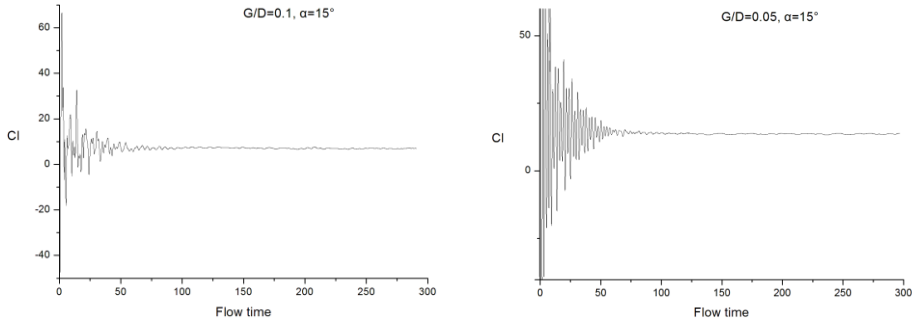

(c) Lift coefficient of G/D=0.10, α=15°. (d) Lift coefficient of G/D=0.05, α=15°.

Figure 5. The lift coefficients of (a) G/D=0.2, α=15 °, (b) G/D=0.15, α=15 °, (c) G/D=0.10, α=15 °, (d) G/D=0.05, α=15 °.

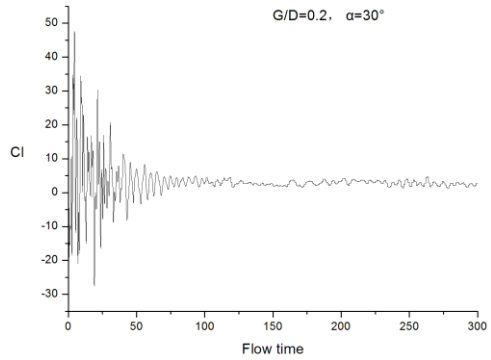

(a) Lift coefficient of G/D=0.20, α=30°.

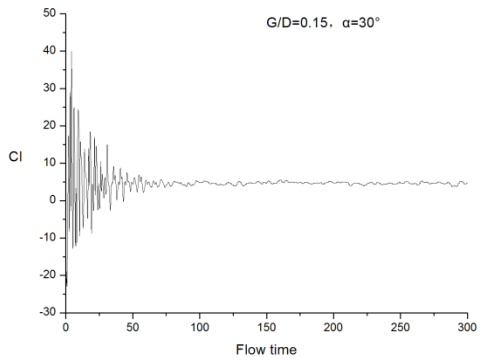

(b) Lift coefficient of G/D=0.15, α=30°.

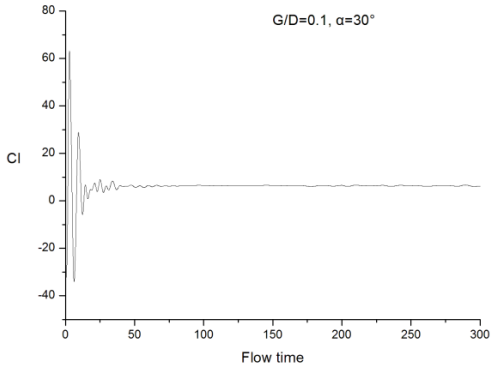

(c) Lift coefficient of G/D=0.10, α=30°.

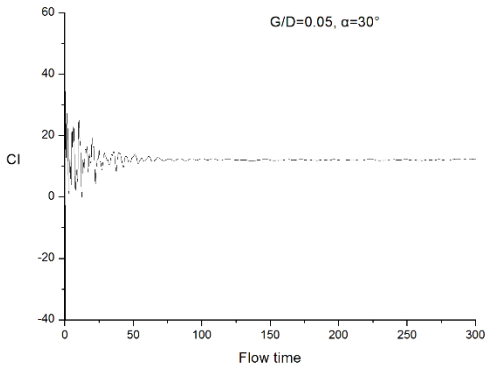

(d) Lift coefficient of G/D=0.05, α=30°.

Figure 6. The lift coefficients of (a) G/D=0.2, α=30 °, (b) G/D=0.15, α=30 °, (c) G/D=0.10, α=30 °, (d) G/D=0.05, α=30 °.

1. The incoming flow with angles of 0^0, 15^0, 30^0 all fully suppresses the vortex shedding at $G/D \le 0.1$.

2. With the gap ratio increase, the effect of the incoming flow angle on vortex shedding suppression becomes obvious, when the gap ratios decrease, the effect of the angle turns to be weak.

3. At critical gap ratios (0.15 to 0.20 in this study), the flow with $\alpha = 15^0$ gives the strongest suppression to the vortex shedding among all the three angles.

REFERENCES

[1] P. W. Bearman and M. M. Zdravkovich, "Flow around a circular cylinder near a plane boundary", *Journal of Fluid Mechanics*, vol. 89, no. 89, pp. 33-47, 1978.

[2] G. Schewe, "On the force fluctuations acting on a circular cylinder in crossflow from subcritical up to transcritical Reynolds numbers", *Journal of Fluid Mechanics*, vol. 133, no. 8, pp. 265-285, 1983.

[3] M. M. Zdravkovich, "Forces on a circular cylinder near a plane wall", *Applied Ocean Research*, vol. 7, no. 4, pp. 197-201, 1985.

[4] S. Taniguchi and K. Miyakoshi, "Fluctuating fluid forces acting on a circular cylinder and interference with a plane wall", *Experiments in Fluids*, vol. 9, no. 4, pp. 197-204, 1990.

[5] C. Lei, L. Cheng, and K. Kavanagh, "Re-examination of the effect of a plane boundary on force and vortex shedding of a circular cylinder", *Journal of Wind Engineering and Industrial Aerodynamics*, vol. 80, no.3, pp. 263-286, 1999.

[6] S. J. Price, D. Sumner, and J. G. Smith, "Flow visualization around a circular cylinder near to a plane wall", *Journal of Fluids and Structures*, vol. 16, no. 2, pp. 175-191, 2002.

[7] X. K. Wang and S. K. Tan, "Near-wake flow characteristics of a circular cylinder close to a wall", *Journal of Fluids and Structures*, vol. 24, no. 5, pp. 605-627, 2008.

[8] Z. P. Zang, F. P. Gao, and J. S. Cui, "Physical modeling and swirling strength analysis of vortex shedding from near-bed piggyback pipelines", *Applied Ocean Research*, no. 40, pp. 50-59, 2013.

[9] C. Lei, L. Cheng, and S. W. Armfield, "Vortex shedding suppression for flow over a circular cylinder near a plane boundary", *Ocean Engineering*, vol. 27, no. 10, pp. 1109-1127, 2000.

[10] A. Dipankar and T. K. Sengupta, "Flow past a circular cylinder in the vicinity of a plane wall", *Journal of Fluids and Structures*, vol. 20, no. 3, pp. 403-423, 2005.

[11] M. Zhao and L. Cheng, "Numerical simulation of two-degree-of-freedom vortex-induced vibration of a circular cylinder close to a plane boundary", *Journal of Fluids and Structures*, vol. 27, no. 7, pp. 1097-1110, 2011.

[12] M. C. Ong, T, Utnes, and L. E. Holmedal, "Numerical simulation of flow around a circular cylinder close to a flat seabed at high Reynolds numbers using a k–ε model", *Coastal Engineering*, vol. 57, no. 10, pp. 931-947, 2010.

[13] M. C. Ong, L. E. Holmedal, and D. Myrhaug, "Numerical simulation of suspended particles around a circular cylinder close to a plane wall in the upper-transition flow regime", *Coastal Engineering*, no. 61, pp. 1-7, 2012.

[14] T. Zhou, H. Wang, S. Rasali, Y. Zhou, and L. Cheng, "Three-dimensional vorticity measurements in the wake of a yawed circular cylinder", *Physics of Fluids*, vol. 22, no. 1, pp. 96-102, 2010.

[15] K. Lam, Y. F. Lin, and L. Zou, "Investigation of turbulent flow past a yawed wavy cylinder", *Journal of Fluids & Structures*, vol. 26, no. 26, pp. 1078-1097, 2010.

[16] J. Thapa, M. Zhao, and T. Zhou, "Three-dimensional simulation of vortex shedding flow in the wake of a yawed circular cylinder near a plane boundary at a Reynolds number of 500", *Ocean Engineering*, vol. 87, no. 9, pp. 25-39, 2014.

[17] A. Ali, R. K. Sharma, and P. Ganesan, "Turbulence model sensitivity and scour gap effect of unsteady flow around pipe: a CFD study", *The scientific world journal*, no. 20, pp. 412136-412136, 2014.

[18] S. C. C. Bailey, M. Vallikivi, and M. Hultmark, "Estimating the value of von Karman's constant in turbulent pipe flow", *Journal of Fluid Mechanics*, vol. 749, no. 79-98, 2014.

[19] M. Zhao, J. Thapa, L. Cheng, and T. Zhou, "Three-dimensional transition of vortex shedding flow around a circular cylinder at right and oblique attacks", *Physics of Fluids*, vol. 25, no. 1, pp. 014105-014105-20, 2013.

[20] Y. Chen, S. Fu, Y. Xu, Q. Zhou, and D. Fan, "Hydrodynamic characters of a near-wall circular cylinder oscillating in cross flow direction in steady current", *Acta Physica Sinica*, vol. 62, no. 6, pp. 675, 2013.